ELSEVIER

Materials Science and Engineering A 495 (2008) 102–107

MATERIALS SCIENCE & ENGINEERING A

www.elsevier.com/locate/msea

# Reactive wetting of Hg–Ag system at room temperature

Avraham Be'er [a], Yossi Lereah [b], Haim Taitelbaum [a,*]

[a] *Department of Physics, Bar-Ilan University, Ramat-Gan 52900, Israel*
[b] *Faculty of Engineering, Tel-Aviv University, Tel-Aviv 69978, Israel*

Received 23 March 2007; received in revised form 6 November 2007; accepted 12 November 2007

**Abstract**

We study the spreading characteristics of a reactive-wetting system of mercury (Hg) droplets on silver (Ag) films at room temperature. Using a recently developed method for reconstructing the dynamical three-dimensional shape of spreading droplets from a microscope top-view, we study the time evolution of the droplet radius and its contact angle. We find that the process consists of two stages: (i) the "bulk propagation" regime, controlled by chemical reaction on the surface, and (ii) the "fast flow" regime which occurs within the metal film as well as on the surface, and consists of both linear (in time) and diffusive propagation. The transition time between the two main time regimes depends solely on the thickness of the Ag film. A final reaction band with an intermetallic compound $Ag_4Hg_3$ is formed in this process. We review our results for the kinetic roughening characteristics of the top-viewed mercury–silver triple line, which is the statistical characterization of the morphology of the triple line, expressed in terms of the growth and roughness scaling exponents. The latter are used to determine the universality class of the system.


*Keywords:* Reactive wetting; Mercury (Hg); Silver (Ag); Reaction band; Kinetic roughening; Growth; Roughness; Universality class

## 1. Introduction

The spreading of liquid droplets on solid surfaces [1–5] is an important process in material science, optics and technology, with a diverse range of applications, e.g. soldering, typing and painting, gluing, condensation of droplets on solid substrates and coating of glasses by photo-resist liquids in photo-lithography processes. The classical wetting process is characterized in terms of the droplet radius $R(t)$, and the contact angle $\theta(t)$, between the droplet and the underlying substrate (Fig. 1a). Theoretical and experimental results for $R(t)$ and $\theta(t)$ show that droplet spreading is usually very slow, with power-law scaling like Tanner's Law, i.e. $R(t) \sim t^{1/10}$ and $\theta(t) \sim t^{-3/10}$ [see Ref. [3] for a review].

When chemical reaction is involved in the wetting process [6–11], the spreading characteristics differ significantly from classical wetting systems. This is due to additional and different mechanisms involved in the process. As a result, in such reactive-wetting systems, $R(t)$ and $\theta(t)$ do not obey a power law. Moreover, a single function cannot describe the full range of $R(t)$ and $\theta(t)$, and their general behavior is a long-standing open question. Landry and Eustathopoulos [9–10], for example, studied the dynamics of reactive-wetting of metallic drops on smooth ceramic surfaces. In their system, a linear spreading regime corresponding to $R(t) \sim t$ was observed for an intermediate part of the spreading process.

In this work we study the time evolving shape (radius and angle) of a mercury droplet spreading on a silver film. This is an interesting example of reactive wetting, that of a room temperature metal-metal/glass compound forming system. Our research is different from traditional reactive-wetting studies by several aspects. First the materials. These specific materials (mercury–silver), which are relevant, e.g. to dentistry [12–14], have not been studied before in the context of spreading processes. Second, since the mercury is one of the few metals which are liquid at room temperature, the experiment can be performed around this temperature, and can be easily observed and monitored using an optical microscope and a CCD camera, within relatively reasonable time scales (a few minutes). In addition, the use of the optical microscope enables us to obtain a dynamical top-view of the process. This feature, combined with fractal analysis concepts of interface growth statistics [15–20], allows us to study the kinetic roughening properties of the triple line.

In order to study the time evolving shape (radius and angle) of the spreading droplet from the two-dimensional top-view

* Corresponding author. Tel.: +972 3 531 8465; fax: +972 3 738 4054.
*E-mail address:* haimt@mail.biu.ac.il (H. Taitelbaum).

0921-5093/$ – see front matter © 2008 Elsevier B.V. All rights reserved.
doi:10.1016/j.msea.2007.11.095

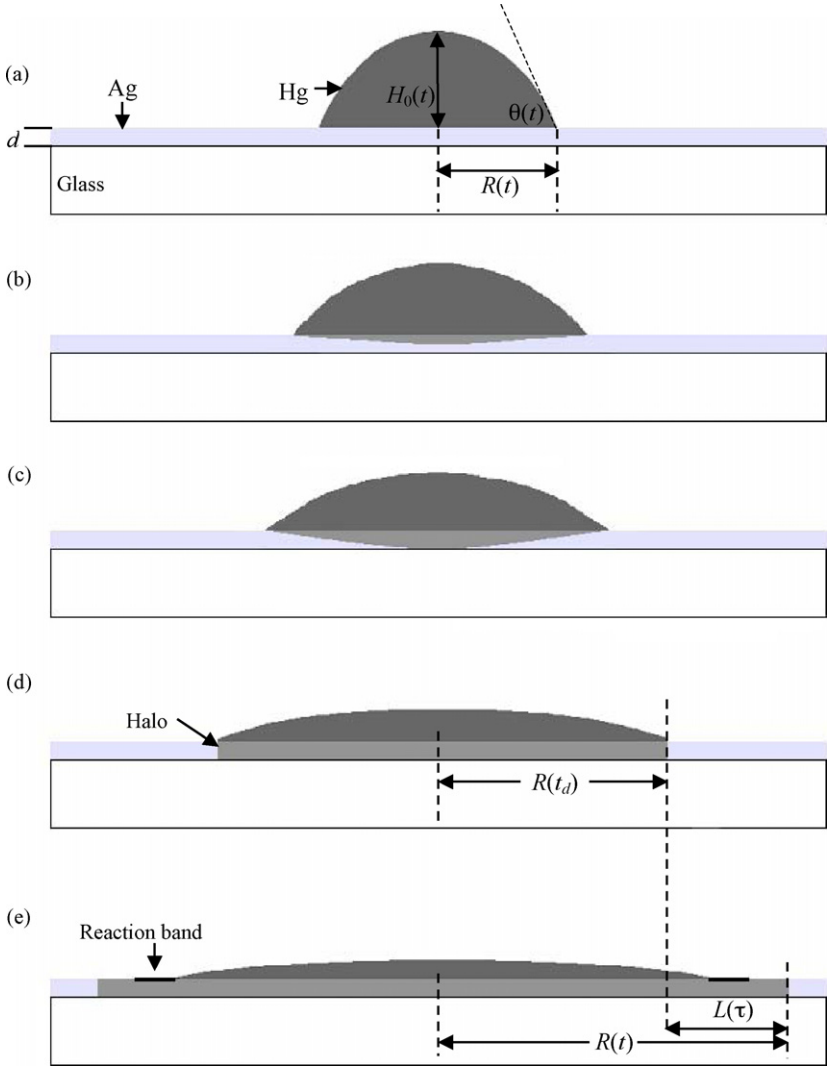


Fig. 1. Schematic sequence of mercury droplet spreading on thin silver films in room temperature. (a) Droplet placement on the film. (b) Droplet spreading and reaction with the underlying substrate. (c) Mercury touching the glass. (d) Starting of the fast-flow regime, halo propagation. (e) Final spreading stage.

images, we used our newly developed experimental method [21], which is based on differential interference contrast (DIC) microscopy. The two-dimensional images provided by the optical microscope consist of different colors, which indicate different slopes in the specimen structure. The color spectrum is calibrated so that each color corresponds to a specific slope/angle of the mercury droplet. It enables one to reconstruct the dynamical three dimensional (3D) structure of tiny (>1 pL), opaque and transparent droplets, with high temporal (0.04 s) and spatial (1 μm) resolution and with an angle resolution of 1°.

The paper is organized as follows. In Section 2 we describe the experimental procedure. In Section 3 we describe the results for the reactive wetting of the droplet bulk. We show that it consists of several time regimes. Initially, the droplet radius grows linearly and the contact angle decreases. This is followed by a fast-flow regime of a precursor-like motion, after a typical crossover time which depends on the thickness of the underlying silver substrate. The fast-flow regime consists of two sub-regimes, a linear propagation [7], with a velocity significantly higher than that of the bulk, which crosses over to a seemingly diffusive motion at the final stages of the process [8,11]. This may be due to different mechanisms, reaction and diffusion, each is dominant in a different sub-region. This part of the paper is based on [22]. In Section 4 we characterize the intermetallic compound forming the reaction band, and in Section 5 we present the fractal analysis of the top-view images of the triple line, based on papers [15–20]. Section 6 is a summary.

## 2. Experimental procedure

The production of smooth, uniform and stable thin metal layers is crucial for successful and reproducible experiments. The Ag (granules 99.99% Chempur) thin films in various thicknesses (200, 300, 350, 380, 420, 500 and 600 nm) were deposited on microscope slides in a slow rate of 0.5 nm/s using standard thermal vacuum deposition. The slides were held in the vacuum chamber at room temperature (no cold finger was used), and the pressure during the evaporation reached $6 \times 10^{-7}$ mbar. Prior to the evaporation, the microscope slides were washed with different solvents – acetone, methanol and isopropanol – each for

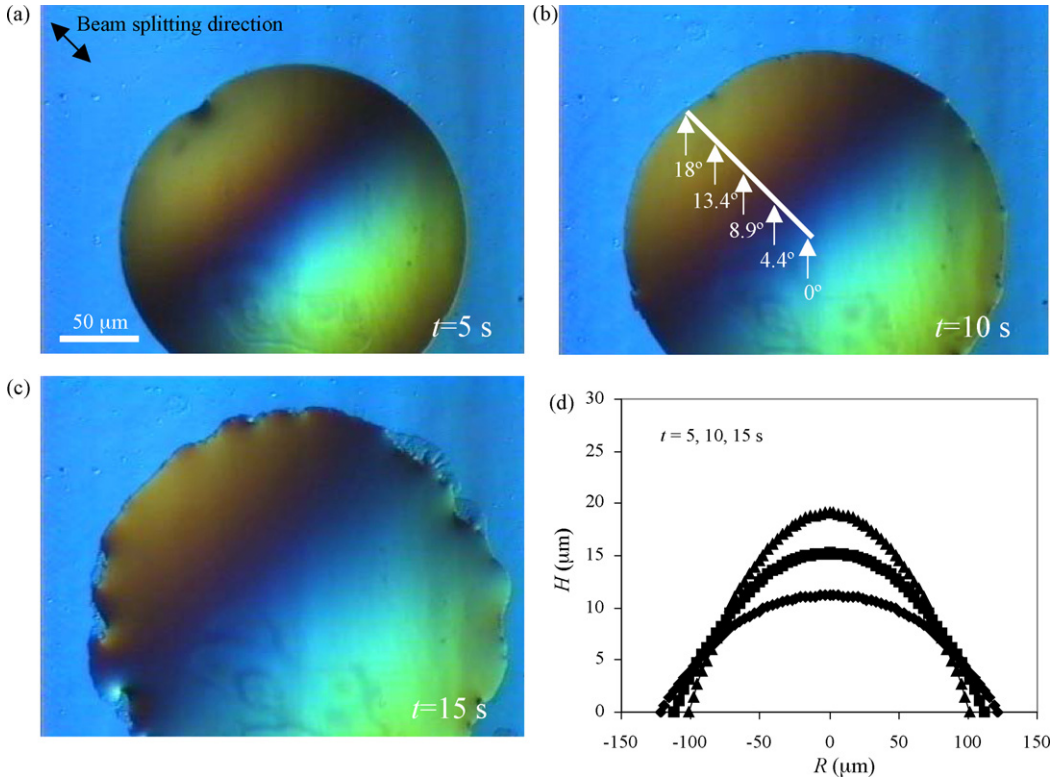


Fig. 2. (a)–(c) Top-view DIC-light-microscopy pictures of Hg droplet spreading on a 420 nm in thickness Ag film, taken at times 5, 10 and 15 s, respectively. The scale bar is 50 μm, and the droplet initial diameter, prior to deposition, is 150 μm. The measurements were taken in a given diametric cross-section of the droplet, parallel to the beam-splitting direction, shown in (a). A typical color-slope calibration is shown on (b). (d) Dynamical side-view of the droplet shape, reconstructed from the top-view pictures (a)–(c).

5 min, using an ultrasonic agitating bath, following by a gentle stream of nitrogen to eliminate the remains of the solvents. The silver was deposited on the microscope slides with no initial deposition of a chromium adhesion layer; no adhesion problems were noted.

Shortly after the evaporation, Hg droplets with initial diameters of 150 μm were carried with a plastic sharp needle, and were placed gently on top of the silver. The droplets were not pushed to the surface but approached the surface until it pulled the droplet by the surface tension forces. The spreading process was monitored using an optical microscope (Axioskop, ZEISS) at room temperature, and was recorded using a high-resolution 3CCD camera. This experiment involves chemical reactions between the solid and the liquid, which create intermetallic compounds such as $Ag_3Hg_4$ and $Ag_4Hg_3$ [12]. The bulk propagation (side-view) was analyzed from the top-view images using the new method. In addition, the propagating triple line (top-view) has been digitized and analyzed in order to study its statistical kinetic roughening properties (see Section 5).

## 3. Bulk and halo propagation

The first stage of the process, the "bulk propagation" regime, lasts for several seconds, depending on the thickness of the Ag film. In this regime, upon placing the droplet on the Ag layer (Fig. 1a), the mercury bulk starts to spread, circularly symmetric, with a smooth contour line (Fig. 1b). In Fig. 2 we show frames taken from an experiment with silver thickness 420 nm. The colors indicate different slopes in the specimen, as is shown in Fig. 2b. The colors evolution with time indicates the dynamic 3D changes. The top-view light-microscope pictures were transformed into projected side-views using the above-mentioned technique. The resulting droplet shape reconstruction is plotted in Fig. 2d.

In Fig. 3, we show the results for the radius $R(t)$ and the angle $\theta(t)$ for the data of Fig. 2. Initially, the droplet radius grows linearly, $R(t) \sim t$, implying a motion of constant velocity, in this case of 2.1 μm/s (Fig. 3a), and the angle of contact $\theta(t)$ decreases continuously (Fig. 3b). At about $t = 15$ s, $\theta(t)$ demonstrates a sudden step in its decreasing trend. As will be shown later, this is the time when the mercury crossed for the first time the entire silver layer, and touched the underlying glass (Fig. 1c). Hence we define this characteristic time as $t_d$, where $d$ is the thickness of the Ag layer. The constant velocity remains approximately the same, with a very slight variation at $t_d$.

Interestingly, the velocity of the bulk propagation is approximately the same for all Ag thicknesses studied, having the average value of $2.5 \pm 0.4$ μm/s. It is reasonable to assume that the velocity does depend, however, on the reaction of the mercury with the silver surface. Indeed, when the silver film is exposed to air prior to the mercury spreading process, the velocity is different, since silver oxidation takes place only on top of the Ag layer [15,19]. It turns out that this surface velocity is much

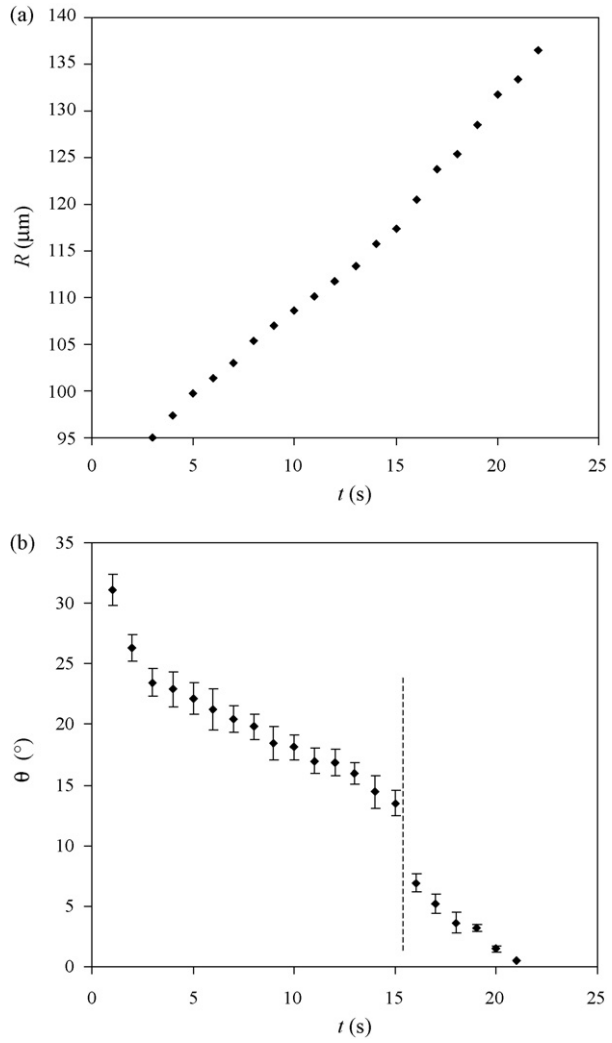


Fig. 3. (a) The radius $R(t)$, and (b) the angle $\theta(t)$, as a function of time, for the bulk propagation regime, for silver thickness of 420 nm. The triple line constant velocity is 2.1 μm/s. At $t_d = 15$ s, $\theta(t)$ demonstrates a sudden step in its decreasing trend.

higher (about two orders of magnitude) than the mercury–silver reaction rate inside the silver film. For example, in the 420 nm system, since the mercury crosses the silver thickness in 15 s, the averaged perpendicular velocity is 420 nm/15 s = 28 nm/s, which is two orders of magnitude smaller than the horizontal velocity 2.1 μm/s. A possible interpretation is that the reaction inside the film is attenuated by another physical mechanism, possibly diffusion. Indeed, the square dependence of $t_d$ on the thickness $d$ [22] supports a diffusion-limited reaction process. Moreover, Lee et al. [13] studied the average interdiffusion coefficient of the gamma phase in the silver–mercury contact reaction, in temperatures slightly above room temperature. They found the interdiffusion coefficient $D$ to be of order $10^{-14}$ m$^2$/s, which agrees with diffusion through 420 nm in 15 s, according to $D \sim (420\,\text{nm})^2/15\,\text{s}$.

The bulk propagation regime does not terminate at $t_d$, but rather extends further in time. However, $t_d$ is the time when another regime, the "fast flow dynamics", shows up. In this regime a new and thin front (~50 nm in height, verified by

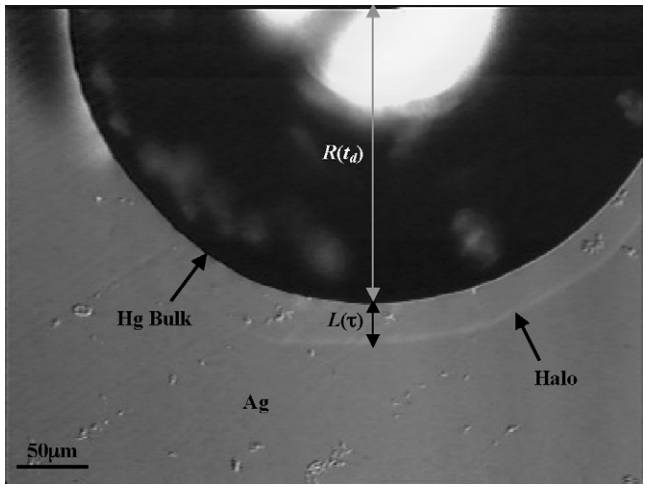


Fig. 4. A top-view, DIC-light-microscopy image of the thin front, which detaches from the bulk and looks like a halo, for Ag thickness of 200 nm. Since this image was taken only 7 TV frames (~0.3 s) after the detachment, $L(\tau)$ is still quite small, compared to $R(t)$. The bulk advancement during this time interval is negligible.

atomic force microscope (AFM)), which optically looks like a halo, detaches from the bulk and flows ahead with a much higher velocity (Fig. 4). We define the propagation distance of this halo as $L(\tau) \equiv R(t) - R(t_d)$, where $R(t)$ and $R(t_d)$ are the distances from the center of the droplet at times $t$ and $t_d$, respectively, and $\tau \equiv t - t_d$ (see Fig. 1d and e). We found that $L(\tau)$ exhibits a crossover behavior in time (Fig. 5), starting from a linear regime $L(\tau) \sim \tau$ at the earlier times (on the $\tau$ scale), followed by a $\tau^{0.4}$ behavior at later times, when the spreading process is slowing down. In the first, linear, reaction-dominated regime, the thickness-dependent velocity is constant, having the values 140, 110 and 40 μm/s, for the 200, 420 and

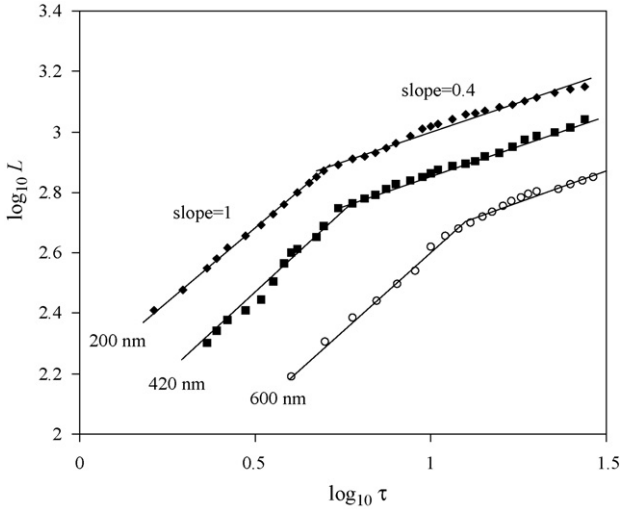


Fig. 5. The propagation of the halo for three different Ag thicknesses. For each thickness, $\tau$ is set to be 0 at a different time, depending on the specific $t_d$. The values of the velocities at the earlier times are 140, 110 and 40 μm/s, for the 200, 420 and 600 nm thicknesses, respectively. For all cases $L(\tau)$ exhibits a crossover behavior in time, starting from a linear regime $L(\tau) \sim \tau$ at the earlier times (on the $\tau$ scale), followed by a $\tau^{0.4}$ behavior at later times.

600 nm thicknesses, respectively. The second regime seems to be diffusion-dominated, with the same time exponent (0.4) for all silver thicknesses (Fig. 5), although the prefactor is different for each case. Similar crossover behaviors between reaction-dominated and diffusion-dominated processes on the surface were reported in Refs. [8,11]. The exponent 0.4 is slightly far from the time exponent 0.5 in standard diffusion, but may still represent a diffusion regime (see also Fig. 7 in Ref. [8]). Alternatively it may reflect a subdiffusive motion (time exponent less than 0.5) whose origin is yet to be studied. The velocity of the halo propagation was found to be significantly higher (1–2 orders of magnitude) than the velocity in the bulk-spreading regime.

The fact that the formation of the faster thin layer that flows ahead of the nominal contact line depends on the Ag thickness, leads us to assume that the glass beneath the Ag film is an important factor in the fast-flow regime. Therefore, we looked at the Ag film from the bottom (the glass slide side). We found that the observed thin Hg layer runs also between the silver and the glass (beneath the silver) in the same structure and velocity that it apparently runs on top [22]. This is sketched in Fig. 1d and e, where the reaction is all over the thin film.

Surprisingly, the time it takes the droplet to cross the Ag layer down to the glass is exactly $t_d$. This suggests that the formation of the new front and the sudden step in $\theta(t)$ are related to the droplet crossing the Ag layer and touching the glass. As the droplet reaches the glass it is not constrained anymore by the surface reaction, because no reaction exists between the Hg and the glass. Consequently, it flows fast through the Ag layer in order to lower the entire system energy. This observation can explain the thickness dependence of the halo velocity at this time regime (Fig. 5).

## 4. Reaction band – intermetallic compound

The fast-flow dynamics gives rise to the formation of a reaction band [8–10], which starts within the fast flow time regime. This band was observed only on the top surface (see Fig. 1e) but not from the bottom view. This band is apparently due to the growth of a new intermetallic phase on top of the film. Scanning electron microscopy (SEM) studies [15] suggest that the new intermetallic compound is $Ag_4Hg_3$. It grows in a structure of islands that can be explained by nucleation and growth mechanisms. The average growth velocity in the spreading direction was found to be that of the bulk propagation, i.e. 2.5 μm/s.

## 5. Kinetic roughening

The kinetic roughening of the Hg–Ag triple line (see, e.g. Fig. 2c), was studied in a series of recent papers [15–20]. It is based on defining a statistical, effective width, for the contact line, as seen by the top-view of the optical microscope (see Fig. 6). This width, which is just the second moment of the front position $h(x,t)$ ($x$ is the location on a segment of length $L$ on the triple line, and $t$ is the time),

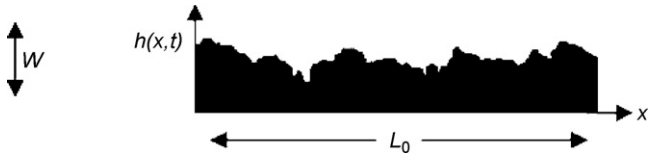


Fig. 6. A schematic sketch of the definition of the statistical width $W$ of a contact line, as the second moment of the front position $h(x,t)$, for a given time.

$$W^2(L,t) = \langle h^2(x,t)\rangle - \langle h(x,t)\rangle^2 \quad (1)$$

obeys an algebraic scaling law,

$$W \sim \begin{cases} t^{\beta} & t \ll t_o \\ L^{\alpha} & t \gg t_o \end{cases} \quad (2)$$

with two scaling exponents, $\alpha$, the roughness exponent and $\beta$, the growth exponent. The crossover time $t_o$ between the two regions is related to the lateral correlation length of the interface line, a length within which a collective motion of the triple line can be assumed. This approach allows one to attribute a statistical universality class to this system. This idea is used for a wide spectrum of interfacial phenomena, ranging, e.g. from slow combustion of paper [23] to penetrating flux fronts in high-$T_c$ thin film superconductors [24].

In order to determine the roughness and growth exponents, one has to digitize and statistically analyze the propagating contact line. We found the exponents to depend on the materials (different exponents for gold films), as well as on the surface substrate (films prepared by other techniques) (see Table 1). For example, AFM studies (Fig. 7) show that gold surface is much smoother than silver surface. As a result, the exponents for gold are much larger. In this sense each system belongs to a different universality class. However, it turns out that that all these systems obey the scaling relation $\alpha + \alpha/\beta = 2$, expected to be valid for isotropic systems. As other possible scaling relations between $\alpha$ and $\beta$ were also predicted (e.g. $\alpha/\beta = 2$, or $\alpha = \beta$, etc.), this seems to be a new tool for classifying reactive-wetting systems according to the top-view data (see, e.g. the top-view images for high temperature wetting in the Au–Sn system [25]).

Using this statistical approach, we recently suggested a new method for extracting the correlation length of the contact line from the width fluctuations of a single interface at relatively earlier stages of the process [18]. Another theoretical work on fluid invasion model shows a possible theoretical relation between the roughness exponent and the wetting properties of the system [26].

Table 1
Summary of roughness and growth exponents

| Material | Thickness | $\alpha$ | $\beta$ |
|---|---|---|---|
| Silver | 200 nm | 0.66 ± 0.03 | 0.46 ± 0.02 |
| | 0.1 mm | 0.77 ± 0.04 | 0.60 ± 0.02 |
| Gold | 150 nm | 0.88 ± 0.03 | 0.76 ± 0.03 |
| | 300 nm | 0.96 ± 0.04 | 1.00 ± 0.04 |

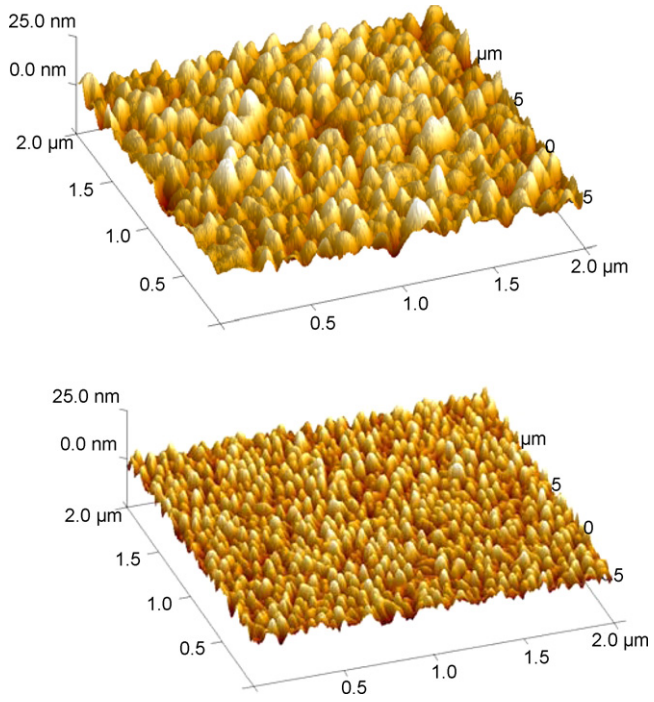


Fig. 7. AFM studies of the surface roughness of thin films. (a) Silver film, thickness 200 nm. Average pin height 20 nm, width 200 nm. (b) Gold film, thickness 150 nm. Average pin height 10 nm, width 100 nm.

## 6. Summary

In this work we studied the spreading of a mercury droplet on a thin silver film in room temperature, using a new, time-resolved optical method. We analyzed the various time regimes of this reactive-wetting system through the time evolution of the radius and the contact angle of the droplet. We observed a remarkable rapid halo propagation, which was observed not only from a top-view but also from a bottom view. This propagation eventually crosses over to diffusive-like growth, due to surface diffusion dominancy at the final stages of the reactive-wetting. We also discussed the statistical aspects of the kinetic roughening of the mercury–silver triple line. This may prove to be an effective probe of the physico-chemical dynamics of the wetting region also in high temperature systems.

## Acknowledgements

We thank Aviad Frydman and Inbal Hecht for fruitful collaboration on this topic.

We thank the Israel Academy of Sciences for financial support, Grant No. 1342/04.

## References

[1] P.G. de Gennes, Rev. Mod. Phys. 57 (1985) 828.
[2] L. Leger, J.F. Joanny, Rep. Prog. Phys. 55 (1992) 431.
[3] A. Oron, S.H. Davis, S.G. Bankoff, Rev. Mod. Phys. 69 (1997) 931.
[4] M.J. de Ruijter, J. De Coninck, T.D. Blake, A. Clarke, A. Rankin, Langmuir 13 (1997) 7293.
[5] M.J. de Ruijter, J. De Coninck, G. Oshanin, Langmuir 15 (1999) 2209.
[6] C.D. Bain, G.M. Whitesides, Langmuir 5 (1989) 1370.
[7] F.G. Yost, F.M. Hosking, D.R. Frear, The Mechanics of Solder-Alloy Wetting and Spreading, Van Nostrand Reinhold, New York, 1993.
[8] H.K. Kim, H.K. Liou, K.N. Tu, J. Mater. Res. 10 (1995) 497.
[9] K. Landry, N. Eustathopoulos, Acta Mater. 44 (1996) 3923.
[10] N. Eustathopoulos, Acta Mater. 46 (1998) 2319.
[11] Y.M. Liu, T.H. Chuang, J. Elect. Mater. 29 (2000) 405.
[12] M. Hansen, Constitution of Binary Alloys, second ed., McGraw-Hill, New York, 1958.
[13] K.H. Lee, M.C. Shin, J.Y. Lee, J. Mater. Sci. 21 (1986) 2430.
[14] M. Levlin, E. Ikavalko, T. Laitinen, Fresenius J. Anal. Chem. 365 (1999) 577.
[15] A. Be'er, Y. Lereah, H. Taitelbaum, Physica A 285 (2000) 156.
[16] A. Be'er, Y. Lereah, I. Hecht, H. Taitelbaum, Physica A 302 (2001) 297.
[17] A. Be'er, Y. Lereah, A. Frydman, H. Taitelbaum, Physica A 314 (2002) 325.
[18] A. Be'er, I. Hecht, H. Taitelbaum, Phys. Rev. E 72 (2005) 031606.
[19] A. Be'er, M.Sc. Thesis, Bar-Ilan University, Ramat-Gan, Israel, 2000.
[20] A. Be'er, Ph.D. Thesis, Bar-Ilan University, Ramat-Gan, Israel, 2005.
[21] A. Be'er, Y. Lereah, J. Microsc. 208 (2002) 148.
[22] A. Be'er, Y. Lereah, A. Frydman, H. Taitelbaum, Phys. Rev. E 75 (2007) 051601.
[23] J. Maunuksela, M. Myllys, O.-P. Kahkonen, J. Timonen, N. Provatas, M.J. Alava, T. Ala-Nissila, Phys. Rev. Lett. 79 (1997) 1515.
[24] R. Surdeanu, R.J. Wijngaarden, E. Visser, J.M. Huijbregtse, J.H. Rector, B. Dam, R. Griessen, Phys. Rev. Lett. 83 (1999) 2054.
[25] L. Yin, S.J. Meschter, T.J. Singler, Acta Mater. 52 (2004) 2873.
[26] I. Hecht, H. Taitelbaum, Phys. Rev. E 70 (2004) 046307.